Journal of Luminescence 215 (2019) 116733

Contents lists available at ScienceDirect

Journal of Luminescence

journal homepage: www.elsevier.com/locate/jlumin

LCOFs: Role of the excited state hydrogen bonding in the detection for nitro-explosives

Yao Xu, Xuedan Song*, Ce Hao

State Key Laboratory of Fine Chemicals, Dalian University of Technology, Dalian, 116024, China

ARTICLE INFO

Keywords:
Luminescent covalent organic frameworks
Nitro-explosives
Hydrogen bonding
Fluorescence quenching
Detection mechanism
TDDFT

ABSTRACT

It is of important theoretical significance to research the mechanism of luminescent covalent organic frameworks (LCOFs) for detecting nitro-explosives. The interaction between LCOF-BTT1 and nitrobenzene has been investigated by DFT and TDDFT methods. By studying electronic configurations and frontier molecular orbitals, the luminescence mechanism of LCOF-BTT1 has changed due to the hydrogen bonding formed between LCOF-BTT1 and nitrobenzene (Complex 1). Further study of electronic transition energies, hydrogen bond lengths, ^{1}H NMR and IR spectra of Complex 1 reveals that hydrogen bonding is stronger in the excited state than in the ground state, indicating fluorescence quenching. Furthermore, the fluorescence rate coefficient and the internal conversion rate coefficient of Complex 1 are correspondingly decreased and increased, indicating that the increase in the strength of hydrogen bonding in the excited state is beneficial to the non-radiative transition and is not conducive to the radiation transition.

1. Introduction

It is of great significance to develop accurate and rapid detection methods for nitro-explosives [1]. Current detection technologies of nitro-explosives include plasma desorption mass spectrometry (PDMS) [2], surface-enhanced Raman spectroscopy (SERS) [3], ion mobility spectrometry (IMS) [4], energy dispersive X-ray diffraction (EDXRD) [5] and so on. In recent years, high-sensitivity, high-selectivity, simple and quick fluorescence detection methods have attracted widespread attention [6–9]. It is worth noting that luminescent covalent organic frameworks (LCOFs) have great application prospects in fluorescence detections due to their strong fluorescence, porosity, good gas permeability, and multiple binding sites [10]. At present, it has been confirmed by experiments that LCOFs can be used to detect substances such as nitro-explosives [11–14], ammonia [15], heavy mental ions [16–18].

However, the mechanism of LCOFs detection for nitro-explosives has not been clearly understood. The causes of fluorescence quenching or enhancement of LCOFs are interactions with substances. When the fluorescence quenching or enhancement effect of the system is reversible, the mechanism of detection is weak interaction such as hydrogen bonding or π-π stacking. Generally, the main interaction between LCOFs and nitro-explosives is hydrogen bonding [19–21]. Many studies have shown that hydrogen bonding is related to the fluorescent properties of luminescent materials [22,23]. The hydrogen bonding not only affects the ground state properties of the material, but also governs the excited state properties of the material. Therefore, the hydrogen bonding behavior in the electronically excited state may have an effect on fluorescent properties of LCOFs. At present, the method of studying excited state hydrogen bonding system in experiment is the time-resolved ultrafast spectroscopy technique [24], whereas this method is difficult to clearly explain ultrafast excited-state processes. In theory, photophysical and photochemical processes of hydrogen bonding systems can be researched by quantum chemical calculations and electronic excited-state hydrogen-bonding dynamics. Under photoexcitation, owing to the difference in charge distributions between different electronic states, the structure of system will be readjusted and the hydrogen bonding system will undergo charge rearrangement, which dynamic process is the electronic excited-state hydrogen bonding dynamic [25]. Zhao et al. [26] elaborated on the study of excited state dynamics of hydrogen-bonding. The time-dependent density functional theory (TDDFT) [27] using in this study has been widely used to calculate excited states of medium molecular systems and is a very reliable method to solve the problem of excited state hydrogen bonding dynamics.

Bojdys et al. [28]used melamine chloride and benzotrithiophene to synthesize LCOF-BTT1 which showed strong blue-green fluorescence under photoexcitation. And the fluorescence of LCOF-BTT1 is quenched when it interacts with nitrobenzene, which has been confirmed by

* Corresponding author.
E-mail address: song@dlut.edu.cn (X. Song).

https://doi.org/10.1016/j.jlumin.2019.116733
Received 17 April 2019; Received in revised form 8 August 2019; Accepted 4 September 2019
Available online 18 September 2019

experiment. Nitrobenzene is a model molecule of nitro-explosives that can be used to study the interaction between LCOF-BTT1 and nitro-explosives. In this research, we have used density functional theory (DFT) and TDDFT to study the difference of luminescence mechanism of LCOF-BTT1 and the hydrogen bonding system (the complex of LCOF-BTT1 and nitrobenzene), to explore the behavior of electronic excited-state hydrogen bonds in the hydrogen bonding system, and explain relationships between electronic excited-state hydrogen bonding behaviors and fluorescent properties of LCOF-BTT1, aiming to understand the mechanism of the fluorescence detection for nitrobenzene by LCOF-BTT1.

2. Computational details

Gaussian16 program package [29] were applied to calculate geometry optimization, frequencies, UV–vis spectra, fluorescence emission spectra, electronic transition energies and ^{1}H NMR. The ground state (S_0 state) and the excited state (S_1 state) of two structures were investigated with DFT and TDDFT methods, respectively. All the computations of two structures were calculated by hybrid exchange–correlation B3LYP-D3 (B3LYP with Grimme's DFT-D3 correction) [30,31] functional and 6-31G(d, p) [32]basis set. In addition, there is a scaling factor of 0.961 for IR spectra [33].

Amsterdam density functional (ADF 2012) program suit [34] was used to obtain frontier molecular orbitals and electronic configurations of two structures with B3LYP-D3 [35] functional and TZP [36] basis set.

MOMAP program developed by Shuai's research group [37] was employed to acquire fluorescence rate coefficients and internal conversion rate coefficients.

3. Results and discussion

3.1. Representative structure of LCOF-BTT1 and hydrogen bonding structure

There is no method that can accurately calculate excited-state periodic systems such as COFs crystals. Hence, we truncated the representative fragment from periodic structure of the 2D LCOF-BTT1 in Fig. 1(a) and truncating bonds were saturated by hydrogen atoms for further desired calculations. The optimized representative fragment structure of LCOF-BTT1 named as Motif is shown in Fig. 1(b). If calculated results of the intercepted structural primitive are consistent with the experimental data of the periodic structure, the reliability of the representative structural Motif can be determined. The structure of the Motif is geometric optimized, and parameters of the structure are listed in Table S1, and IR spectra, UV–Vis spectra and fluorescence spectra are shown in Fig. 2(a), Fig. 2(b) and (c), respectively. The calculated IR spectra, the maximum absorption peak of UV–Vis spectra and the maximum emission peak of fluorescence spectra are in good agreement with the corresponding experimental data. The consistency of vibrational structures and electronic structures indicates the Motif is reliability and can instead of the periodic LCOF-BTT1 for further calculations.

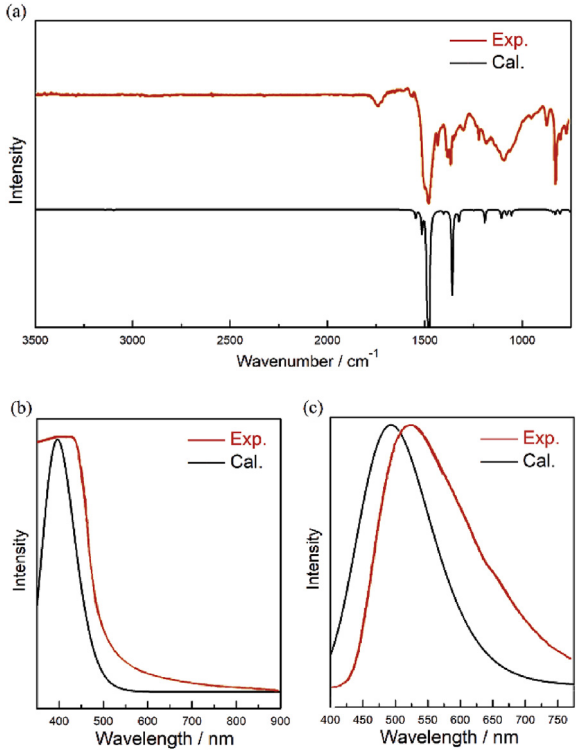

Fig. 2. Comparisons of experimental and computational IR spectra (a), UV–Vis spectra (b) and fluorescence spectra (c) for LCOF-BTT1.

Addition of a molecule of nitrobenzene to Motif results in a hydrogen bonding system. As a result of there being multiple potential sites in the truncated structure of LCOF-BTT1 at which hydrogen bonding could form, we assembled several different structures and got three different hydrogen bonding complexes shown in Fig. S2. Comparing energies of these different complexes (Table S2), we labelled the most stable of these as Complex 1 which is shown in Fig. 1(c) as the computational model.

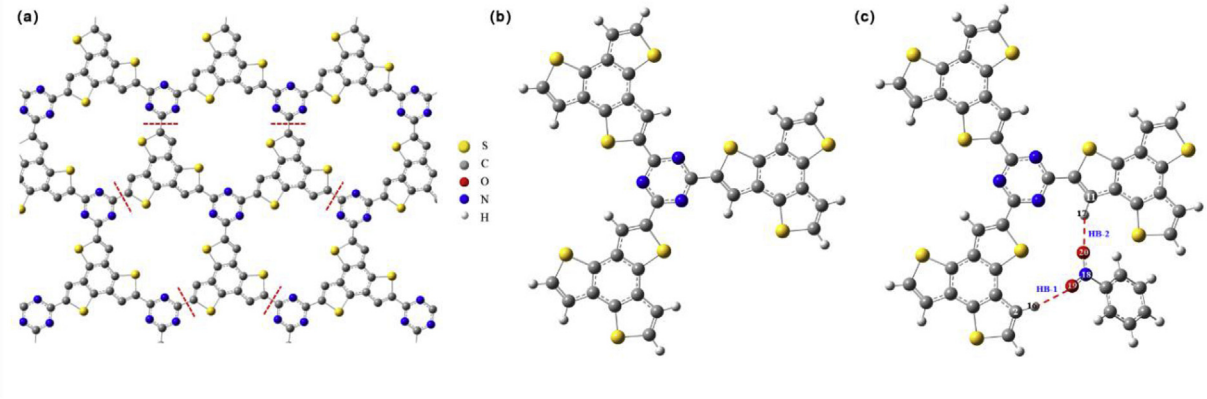

Fig. 1. (a) The periodic structure of LCOF-BTT1 where truncated by the red dotted lines; (b)The optimized geometric structure of Motif; (c) The most stable hydrogen bonding system donated as Complex 1 which is formed by LCOF-BTT1 and nitrobenzene. (For interpretation of the references to colour in this figure legend, the reader is referred to the Web version of this article.)

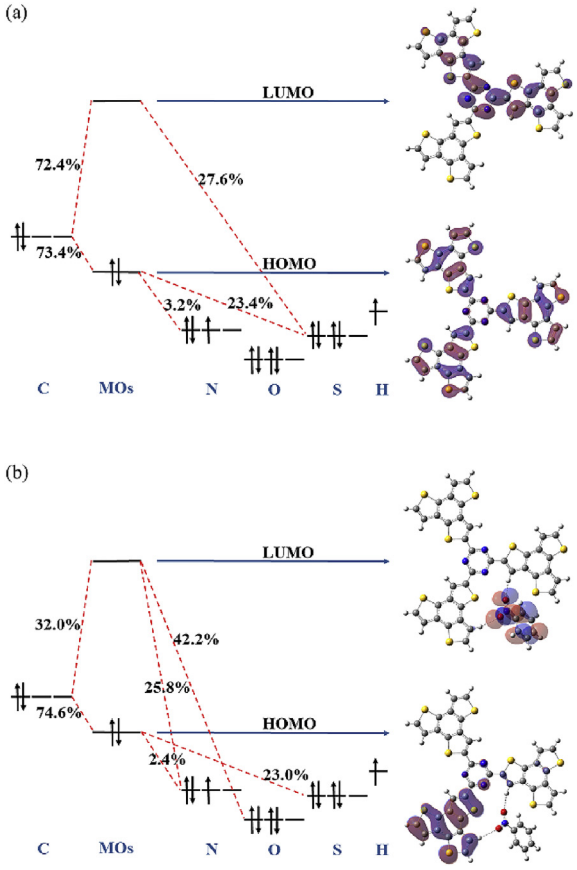

Fig. 3. Electronic configurations and frontier molecular orbitals of (a) Motif and (b) Complex 1, respectively.

3.2. Electronic configurations and frontier molecular orbitals

According to the Kasha's rule [38], appreciable fluorescence quantum yields only occurs in the lowest excited state (S_1 state). Therefore, exploring electron transition from the S_1 state to the S_0 state via electronic configurations and frontier molecular orbitals of Motif and Complex 1 (Fig. 3) investigates the influence of hydrogen bonding on this system. Fig. 3(a) reveals that, with respect of Motif, electron density distributions of LUMO and HOMO are predominantly localized on the cyanuric group and benzotrithiophene group, respectively. LUMO is mainly composed of 72.4% carbon atoms and 27.6% sulphur atoms; HOMO mainly consists of 73.4% carbon atoms, 23.4% sulphur atoms and 3.2% nitrogen atoms. From this, we can conclude that the luminescence mechanism of LCOF-BTT1 should be attributed to ligand-to-ligand charge transfer (LLCT).

The calculated electronic configurations and frontier molecular orbitals of Complex 1 show in Fig. 3(b). LUMO of the Complex 1 is mainly composed of 42.2% oxygen atoms, 32.0% carbon atoms and 25.8% nitrogen atoms in nitrobenzene; HOMO mainly consists of 73.4% carbon atoms, 23.4% sulphur atoms and 3.2% nitrogen atoms. It can be seen that electronic density distributions of HOMO locate on ligands whereas those of LUMO locate on nitrobenzene. This demonstrates that the luminescence mechanism of Complex 1 is ligand-to-guest charge transfer. We can conclude that the formation of hydrogen bonding between nitrobenzene and LCOF-BTT1 has significance influence on the luminescence properties of the LCOF-BTT1.

3.3. Electronic transition energies

Hydrogen bonding interaction has a significant impact on the electron excitation process. After photoinduced electron excitation, hydrogen bonding systems have obvious difference about electronic density distributions in different electronic states, thereupon the excitation energy of each electronic state also changes. Therefore, changes of electronic transition energies can illustrate hydrogen bonding behaviors in the excited state. When the electron spectrum is red-shifted, it reveals that hydrogen bonding is enhanced in the excited state. On the contrary, the blue-shifted of the electron spectrum indicates that the hydrogen bonding is weakened in the excited state [26,39]. Electronic transition energies of Motif and Complex 1 are listed in Table 1. It clearly shows that transition energies of Complex 1 are lower than Motif. Thus, we speculate that the hydrogen bonding is strengthened in the S_1 state.

Table 1
Calculated electronic transition energies of Motif and Complex 1 in different excited states.

Excited states	Motif / eV	Complex 1 / eV
S_1	3.08	2.30
S_2	3.13	2.34
S_3	3.13	2.45
S_4	3.17	2.50
S_5	3.17	2.66
S_6	3.19	2.71
S_7	3.21	3.08
S_8	3.21	3.12
S_9	3.22	3.15
S_{10}	3.25	3.16

3.4. The behavior of hydrogen bonding in the S_1 state

There are some criteria to demonstrate the hydrogen bonding behavior via changes of hydrogen bond lengths, hydrogen atom chemical shifts and vibrational frequencies of hydrogen donor and acceptor groups from the S_0 state to the S_1 state. If the hydrogen bond lengths become shorter, ^{1}H NMR of the hydrogen proton donors moves to upfield and vibration frequencies of hydrogen donor and acceptor groups are red-shifted, these illuminate that the electronic excited-state hydrogen bonding is strengthened [26,40–42].

We calculated geometry optimization, frequencies and ^{1}H NMR of the hydrogen bonding Complex 1 in the S_0 state and S_1 state, respectively. Hydrogen bond lengths and hydrogen atom ^{1}H NMR of Complex 1 in the S_0 state and S_1 state are listed in Table 2. Comparing the geometry optimization of Complex 1 in the S_0 state and S_1 state, the length of hydrogen bond N18–O19···H16–C2 (HB-1) shortens evidently from 2.39 Å to 1.96 Å and the length of hydrogen bond N18–O20···H17–C11 (HB-2) shortens from 2.36 Å to 2.28 Å. It means that hydrogen bonds of Complex 1 are strengthened in the S_1 state. Furthermore, hydrogen atom chemical shifts associate with changes of hydrogen bonds. From Table 2, ^{1}H NMR of H16 decreases from 23.40 ppm to 22.67 ppm and ^{1}H NMR of H17 decreases from 21.64 ppm to 21.38 ppm in the S_1 state. Since the H16 and the H17 chemical shifts decrease evidently from the S_0 state to the S_1 state, shielding effect is strengthening and charge densities around hydrogen nucleuses are increasing. It illustrates that hydrogen acceptors are closer to H atoms and

Table 2
Calculated hydrogen bond lengths and hydrogen atom chemical shifts of Complex 1 in the S_0 State and the S_1 State.

	S_0	S_1
HB length / Å		
HB-1 (N18–O19···H16–C2)	2.39	1.96
HB-2 (N18–O20···H17–C11)	2.36	2.28
^{1}H NMR / ppm		
H16	23.40	22.67
H17	21.64	21.38

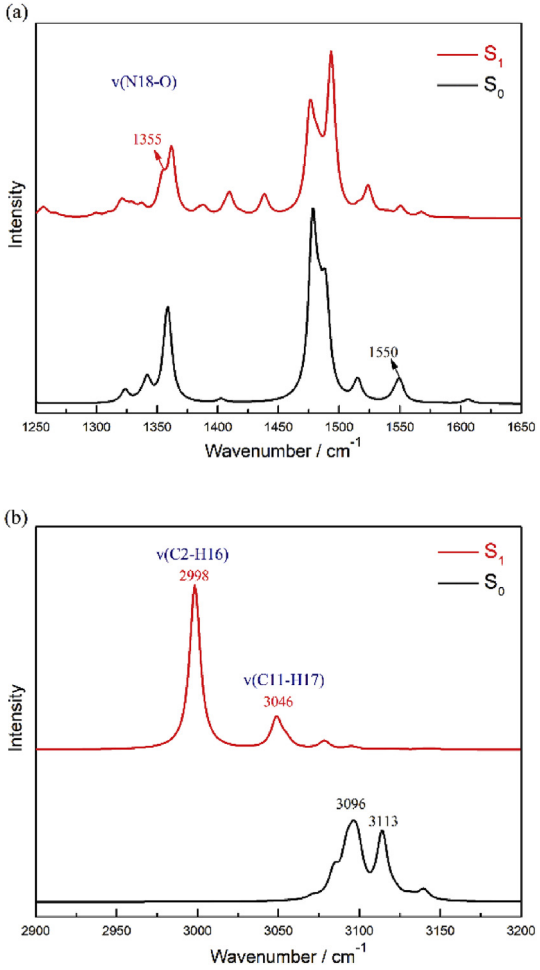

Fig. 4. Stretching vibration frequencies of (a) N=O and (b) C2–H16 and C11–H17 in the S_0 state (black) and S_1 state (red). (For interpretation of the references to colour in this figure legend, the reader is referred to the Web version of this article.)

excited-state hydrogen bonds of Complex 1 are strengthened.

The changes of hydrogen bond strength lead to chemical bond strength of hydrogen donor and acceptor groups changing which is related to vibration frequencies. Therefore, hydrogen bonding behaviors can be studied through comparing the characteristic vibration frequencies of hydrogen donor and acceptor groups in the ground state and the excited state. If the vibration frequencies of hydrogen donor and acceptor groups in S_0 state are red-shifted relative to the S_1 state, the excited-state hydrogen bonds are enhanced. On the contrary, if the characteristic vibration frequencies of hydrogen donor and acceptor groups in S_0 state are blue-shifted relative to the S_1 state, it shows that the excited-state hydrogen bonds are weakened [26]. Fig. 4(a) and (b) display the vibrational regions of the N=O and C–H stretching frequencies coming from IR spectra of Complex 1 in the S_0 state and S_1 state. It is obvious that there are red-shifts of C2–H16 stretching frequency from 3096 cm^{-1} to 2998 cm^{-1} and C11–H17 stretching frequency from 3113 cm^{-1} to 3046 cm^{-1}. Moreover, N=O stretching frequency also displays a red-shifted from 1550 cm^{-1} to 1355 cm^{-1}. Consequently, red-shifted of N=O and C–H stretching frequencies in the S_1 state reveal that the excited-state hydrogen bonding of Complex 1 is strengthened.

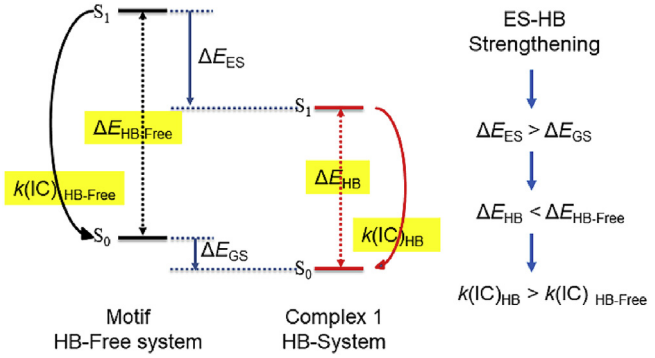

Fig. 5. The schematic diagram of the relationship between hydrogen bonds strengthening and luminescent properties of LCOF-BTT1 in the excited state.

3.5. The relationship between the hydrogen bonding behavior and fluorescence of LCOF-BTT1 in the excited state

From the above, results of electronic configurations and frontier molecular orbitals indicate that hydrogen bonding between LCOF-BTT1 and nitrobenzene influences the luminescence mechanism of LCOF-BTT1. Moreover, decreases of hydrogen bond lengths, upfield shifting of hydrogen atom ^{1}HNMR and red-shifts of hydrogen donor and acceptor groups vibrational frequencies demonstrate that hydrogen bonds are strengthened in the excited state. Comparing electronic transition energies of Motif and Complex 1, excited state hydrogen bonds strengthening causes energy level in the S_1 state lower than in the S_0 state ($\Delta E_{ES} > \Delta E_{GS}$). Thereby, the electronic transition energy of hydrogen bonding Complex 1 is below than hydrogen bond-free Motif ($\Delta E_{HB} < \Delta E_{HB\text{-}Free}$), as shown in Fig. 5. Thus, strengthening of excited-state hydrogen bonds leads to electron coupling enhancement between nitrobenzene and LCOF-BTT1, which is beneficial to the occurrence of photoinduced electron transfer and enhancing of internal conversion between the S_0 state and the S_1 state ($k(IC)_{HB} > k(IC)_{HB\text{-}Free}$) [43]. Furthermore, non-radiative transition internal conversion and radiative transition fluorescence competes with each other and the enhancement of internal conversion results in fluorescence weakening. Consequently, strengthening of hydrogen bonding in the excited state leads to fluorescence weakening or quenching of LCOF-BTT1.

Since the calculated fluorescence rate coefficient can correspond to the experimentally measured fluorescence intensity, we calculated fluorescence rate coefficients and internal conversion rate coefficients of Motif and Complex 1, respectively. Basing on the Fermi's Golden rule, quantum chemical calculations can be employed to predict rate coefficients of various deactivation processes such as fluorescence and internal conversion. Taking time-dependent perturbation theory and Franck-Condon approximation into account, the fluorescence rate coefficient (k_F) [44] can be expressed as

$$k_F = \int_0^{+\infty} \frac{4\omega^3}{3\hbar c^2} |\overrightarrow{\mu_0}|^2 \sum_{v_i,v_f} P_{i,v_i}(T) |\langle \Theta_{fv_f}|\Theta_{iv_i}\rangle|^2 \delta(\omega_{iv_i,fv_f} - \omega) d\omega \quad (1)$$

In addition, the rate coefficient of internal conversion (k_{IC}) [45] can be expressed as

$$k_{IC} = \frac{2\pi}{\hbar} \sum_{v_i,v_f} P_{i,v_i}(T) \left| \sum_n \langle \Phi_f|\hat{P}_n|\Phi_i\rangle \langle \Theta_{f,v_f}|\hat{P}_n|\Theta_{i,v_i}\rangle \right|^2 \delta(E_{i,v_i} - E_{f,v_f}) \quad (2)$$

In equation, ω is the angular frequency; υ is vibrational mode; c is light speed in vacuum; $\overrightarrow{\mu_0}$ is the electronic transition dipole moment; T is temperature; $P_{i,v_i}(T)$ represents the Boltzmann distribution function of the initial vibronic manifold; i and f represent the initial and final states, respectively; δ is Dirac operator; Θ and Φ represent vibrational and electronic wave functions, respectively; n is the index of normal mode and $\hat{P}_n$ represents the momentum operator of the n th normal

Table 3
Calculated fluorescence rate coefficients (k_F) and internal conversion rate coefficients (k_{IC}) of Motif and Complex 1.

Rate coefficients	Motif	Complex 1
k_F / s^{-1}	1.36×10^5	8.44×10^4
k_{IC} / s^{-1}	5.16×10^9	1.00×10^{11}

mode in the final electronic state.

As shown in Table 3, the k_F of Complex 1 is less than Motif and the conversion rate k_{IC} of Complex 1 is more than Motif. The calculated fluorescence rate coefficient of the complex of LCOF-BTT1 and nitrobenzene is reduced by half. This is consistent with the experimentally measured decrease in fluorescence intensity, so the experimental results can support computed results. The calculations also present that internal conversion of Complex 1 plays a main role in the process from the S_1 state to the S_0 state and the process of fluorescence is weakened or quenched. Thus, excited-state hydrogen bonds strengthening can influence on fluorescence properties of LCOF-BTT1.

From the qualitative and quantitative analysis, all of conclusions demonstrate the luminescence mechanism of LCOF-BTT1 changes fundamentally after hydrogen bonding with nitrobenzene and hydrogen bonds strengthening results in internal conversion enhancing which is the essence of fluorescence weakening or quenching. Therefore, it illuminates that the enhancement of electronic excited-state hydrogen bonding is the fundamental reason why LCOF-BTT1 can detect nitrobenzene.

4. Conclusion

We report a new understanding of the fluorescence detection mechanism for nitro-explosives by LCOF-BTT1. From detailed theoretical investigation of the hydrogen bonding interaction between nitrobenzene and the representative fragment of LCOF-BTT1 crystal, the following important conclusions are obtained: (1) Analysis of the frontier molecular orbitals and electronic configuration indicates that changes in luminescence should be attributed to hydrogen bonding. (2) The calculated electronic transition energies of Complex 1 are lower than Motif, indicating that the hydrogen bonding between nitrobenzene and LCOF-BTT1 is strengthened upon excitation. (3) Comparison of bond lengths, ^{1}H NMR chemical shifts and vibrational frequencies in the S_0 and S_1 states indicates that the intermolecular hydrogen bonds HB-1 and HB-2 are strengthened in the S_1 state, which is likely to induce fluorescence quenching. Therefore, hydrogen bonding is enhanced in the electronic excited state which is beneficial to the non-radiative transition and not beneficial to the radiation transition, explaining the mechanism for detecting nitro-explosives by LCOF-BTT1. Our work also provides a potential approach for controlling of luminescent properties of LCOFs by hydrogen bonding, and further studies should be launched in this area to promote practical applications of luminescent COFs.

Acknowledgements

This work was supported by National Natural Science Foundation of China (Grant Nos. 21606040 and 21677029), the Fundamental Research Funds for the Central Universities, China (DUT18LK26).

Appendix A. Supplementary data

Supplementary data to this article can be found online at https://doi.org/10.1016/j.jlumin.2019.116733.

References

[1] Y. Salinas, R. Martinez-Manez, M.D. Marcos, F. Sancenon, A.M. Costero, M. Parra, S. Gil, Optical chemosensors and reagents to detect explosives, Chem. Soc. Rev. 41 (2012) 1261–1296 http://doi.org/10.1039/c1cs15173h.
[2] K. Håkansson, R.V. Coorey, R.A. Zubarev, V.L. Talrose, P. Håkansson, Low-mass ions observed in plasma desorption mass spectrometry of high explosives, J. Mass Spectrom. 35 (2015) 337–346.
[3] G. Ping, D. Gosztola, M.J. Weaver, Surface-enhanced Raman-spectroscopy as a probe of electroorganic reaction pathways .1. Processes involving adsorbed nitrobenzene, azobenzene and related species, J. Phys. Chem. 92 (1988) 7122–7130.
[4] W. Lu, H. Li, Z. Meng, X. Liang, M. Xue, Q. Wang, X. Dong, Detection of nitrobenzene compounds in surface water by ion mobility spectrometry coupled with molecularly imprinted polymers, J. Hazard Mater. 280 (2014) 588–594 http://doi.org/10.1016/j.jhazmat.2014.08.041.
[5] R.D. Luggar, M.J. Farquharson, J.A. Horrocks, R.J. Lacey, Multivariate analysis of statistically poor EDXRD spectra for the detection of concealed explosives, X Ray Spectrom. 27 (1998) 87–94.
[6] S.W. Thomas, G.D. Joly, T.M. Swager, Chemical sensors based on amplifying fluorescent conjugated polymers, Chem. Rev. 107 (2007) 1339–1386 http://doi.org/10.1021/cr0501339.
[7] X. Liu, Y. Xu, D. Jiang, Conjugated microporous polymers as molecular sensing devices: microporous architecture enables rapid response and enhances sensitivity in fluorescence-on and fluorescence-off sensing, J. Am. Chem. Soc. 134 (2012) 8738–8741 http://doi.org/10.1021/ja303448r.
[8] Z. Hu, B.J. Deibert, J. Li, Luminescent metal-organic frameworks for chemical sensing and explosive detection, Chem. Soc. Rev. 43 (2014) 5815–5840 http://doi.org/10.1039/c4cs00010b.
[9] W.P. Lustig, S. Mukherjee, N.D. Rudd, A.V. Desai, J. Li, S.K. Ghosh, Metal-organic frameworks: functional luminescent and photonic materials for sensing applications, Chem. Soc. Rev. 46 (2017) 3242–3285 http://doi.org/10.1039/c6cs00930a.
[10] R. Xue, H. Guo, T. Wang, L. Gong, Y. Wang, J. Ai, D. Huang, H. Chen, W. Yang, Fluorescence properties and analytical applications of covalent organic frameworks, Anal. Methods 9 (2017) 3737–3750 http://doi.org/10.1039/c7ay01261f.
[11] G. Lin, H. Ding, D. Yuan, B. Wang, C. Wang, A pyrene-based, fluorescent three-dimensional covalent organic framework, J. Am. Chem. Soc. 138 (2016) 3302–3305 http://doi.org/10.1021/jacs.6b00652.
[12] S. Dalapati, S. Jin, J. Gao, Y. Xu, A. Nagai, D. Jiang, An azine-linked covalent organic framework, J. Am. Chem. Soc. 135 (2013) 17310–17313 http://doi.org/10.1021/ja4103293.
[13] W. Zhang, L.G. Qiu, Y.P. Yuan, A.J. Xie, Y.H. Shen, J.F. Zhu, Microwave-assisted synthesis of highly fluorescent nanoparticles of a melamine-based porous covalent organic framework for trace-level detection of nitroaromatic explosives, J. Hazard Mater. 221–222 (2012) 147–154 http://doi.org/10.1016/j.jhazmat.2012.04.025.
[14] D. Kaleeswaran, P. Vishnoi, R. Murugavel, [3+3] Imine and β-ketoenamine tethered fluorescent covalent-organic frameworks for CO2 uptake and nitroaromatic sensing, J. Mater. Chem. C 3 (2015) 7159–7171 http://doi.org/10.1039/c5tc00670h.
[15] S. Dalapati, E. Jin, M. Addicoat, T. Heine, D. Jiang, Highly emissive covalent organic frameworks, J. Am. Chem. Soc. 138 (2016) 5797–5800 http://doi.org/10.1021/jacs.6b02700.
[16] E. Özdemir, D. Thirion, C.T. Yavuz, Covalent organic polymer framework with C–C bonds as a fluorescent probe for selective iron detection, RSC Adv. 5 (2015) 69010–69015 http://doi.org/10.1039/c5ra10697d.
[17] S.Y. Ding, M. Dong, Y.W. Wang, Y.T. Chen, H.Z. Wang, C.Y. Su, W. Wang, Thioether-based fluorescent covalent organic framework for selective detection and facile removal of Mercury(II), J. Am. Chem. Soc. 138 (2016) 3031–3037 http://doi.org/10.1021/jacs.5b10754.
[18] Z. Li, Y. Zhang, H. Xia, Y. Mu, X. Liu, A robust and luminescent covalent organic framework as a highly sensitive and selective sensor for the detection of Cu(2+) ions, Chem. Commun. 52 (2016) 6613–6616 http://doi.org/10.1039/c6cc01476c.
[19] L. Liu, X. Chen, J. Qiu, C. Hao, New insights into the nitroaromatics-detection mechanism of the luminescent metal-organic framework sensor, Dalton Trans. 44 (2015) 2897–2906 http://doi.org/10.1039/c4dt03185g.
[20] P. Wang, X. Song, Z. Zhao, L. Liu, W. Mu, C. Hao, Role of the electronic excited-state hydrogen bonding in the nitro-explosives detection by [Zn 2 (oba) 2 (bpy)], Chem. Phys. Lett. 661 (2016) 257–262 http://doi.org/10.1016/j.cplett.2016.06.085.
[21] Z. Zhao, X. Song, L. Liu, G. Li, S. Shah, C. Hao, A recognition mechanism study: luminescent metal-organic framework for the detection of nitro-explosives, J. Mol. Graph. Model. 80 (2018) 132–137 http://doi.org/10.1016/j.jmgm.2017.12.024.
[22] Y. Yao, X. Song, J. Qiu, C. Hao, Interaction between formaldehyde and luminescent MOF [Zn(NH(2)bdc)(bix)]n in the electronic excited state, J. Phys. Chem. A 118 (2014) 6191–6196 http://doi.org/10.1021/jp503722m.
[23] Z. Zhao, J. Hao, X. Song, S. Ren, C. Hao, A sensor for formaldehyde detection: luminescent metal–organic framework [Zn2(H2L)(2,2′-bpy)2(H2O)]n, RSC Adv. 5 (2015) 49752–49758 http://doi.org/10.1039/c5ra07373a.
[24] G. Zhao, J. Liu, L. Zhou, K. Han, Site-selective photoinduced electron transfer from alcoholic solvents to the chromophore facilitated by hydrogen bonding: a new fluorescence quenching mechanism, J. Phys. Chem. B 111 (2007) 8940–8945 http://doi.org/10.1021/jp0734530.
[25] G. Zhao, K. Han, Early time hydrogen-bonding dynamics of photoexcited coumarin 102 in hydrogen-donating solvents: theoretical study, J. Phys. Chem. A 111 (2007) 2469–2474 http://doi.org/10.1021/jp068420j.
[26] G. Zhao, K. Han, Hydrogen bonding in the electronic excited state, Acc. Chem. Res. (2012) 404–413, https://doi.org/10.1021/ar200135h.
[27] E. Runge, E.K.U. Gross, Density-functional theory for time-dependent systems, Phys. Rev. Lett. 52 (1984) 997–1000 http://doi.org/10.1103/PhysRevLett.52.997.
[28] Y.S. Kochergin, D. Schwarz, A. Acharjya, A. Ichangi, R. Kulkarni, P. Eliasova, J. Vacek, J. Schmidt, A. Thomas, M.J. Bojdys, Exploring the "Goldilocks Zone" of

semiconducting polymer photocatalysts by donor-acceptor Interactions, Angew. Chem. Int. Ed. 57 (2018) 14188–14192 http://doi.org/10.1002/anie.201809702.
[29] R.A. Gaussian 16, G.W.T.M.J. Frisch, H.B. Schlegel, G.E. Scuseria, J.R.C.M.A. Robb, G. Scalmani, V. Barone, H.N.G.A. Petersson, X. Li, M. Caricato, A.V. Marenich, B.G.J.J. Bloino, R. Gomperts, B. Mennucci, H.P. Hratchian, A.F.I.J.V. Ortiz, J.L. Sonnenberg, D. Williams-Young, F.L.F. Ding, F. Egidi, J. Goings, B. Peng, A. Petrone, D.R.T. Henderson, V.G. Zakrzewski, J. Gao, N. Rega, W.L.G. Zheng, M. Hada, M. Ehara, K. Toyota, R. Fukuda, M.I.J. Hasegawa, T. Nakajima, Y. Honda, O. Kitao, H. Nakai, K.T.T. Vreven, J.A. Montgomery Jr., J.E. Peralta, M.J.B.F. Ogliaro, J.J. Heyd, E.N. Brothers, K.N. Kudin, T.A.K.V.N. Staroverov, R. Kobayashi, J. Normand, A.P.R.K. Raghavachari, J.C. Burant, S.S. Iyengar, M.C.J. Tomasi, J.M. Millam, M. Klene, C. Adamo, R. Cammi, R.L.M.J.W. Ochterski, K. Morokuma, O. Farkas, D.J.F.J.B. Foresman, Gaussian, Inc. Wallingford CT (2016).
[30] A.D. Becke, A new mixing of Hartree–Fock and local density-functional theories, J. Chem. Phys. 98 (1993) 1372–1377 http://doi.org/10.1063/1.4869598.
[31] G. Stefan, E. Stephan, G. Lars, Effect of the damping function in dispersion corrected density functional theory, J. Comput. Chem. 32 (2011) 1456–1465.
[32] M.M. Francl, W.J. Pietro, W.J. Hehre, J.S. Binkley, M.S. Gordon, D.J. Defrees, J.A. Pople, Self-consistent molecular orbital methods. XXIII. A polarization-type basis set for second-row elements, J. Chem. Phys. 77 (1982) 3654–3665.
[33] D. Russell, Johnson III (Eds.), NIST computational chemistry Comparison and benchmark database NIST standard reference database number 101 release 19, 2018 http://cccbdb.nist.gov/.
[34] F.M.B.G. te Velde, E.J. Baerends, C. Fonseca Guerra, S.J.A. vanGisbergen, J.G. Snijders, T. Ziegler, Chemistry with ADF, J. Comput. Chem. 22 (2001) 931–967.
[35] G. Stefan, A. Jens, E. Stephan, K. Helge, A consistent and accurate ab initio parametrization of density functional dispersion correction (DFT-D) for the 94 elements H-Pu, J. Chem. Phys. 132 (2010) 154104 http://doi.org/10.1063/1.3382344.
[36] E. Lenthe, Van, E.J. Baerends, Optimized Slater-type basis sets for the elements 1-118, J. Comput. Chem. 24 (2003) 1142–1156.
[37] Y. Niu, W. Li, P. Qian, G. Hua, Y. Yi, L. Wang, G. Nan, W. Dong, Z. Shuai, MOlecular MAterials Property Prediction Package (MOMAP) 1.0: a software package for predicting the luminescent properties and mobility of organic functional materials, Mol. Phys. 116 (2018) 1–13.
[38] M. Kasha, Characterization of electronic transitions in complex molecules, Discuss. Faraday Soc. 9 (1950) 14–19.
[39] G. Zhao, B.H. Northrop, K. Han, P.J. Stang, The effect of intermolecular hydrogen bonding on the fluorescence of a bimetallic platinum complex, J. Phys. Chem. A 114 (2010) 9007–9013 http://doi.org/10.1021/jp105009t.
[40] Y. Liu, J. Ding, D. Shi, J. Sun, Time-dependent density functional theory study on electronically excited States of coumarin 102 chromophore in aniline solvent: reconsideration of the electronic excited-state hydrogen-bonding dynamics, J. Phys. Chem. A 112 (2008) 6244–6248 http://doi.org/10.1021/jp8022919.
[41] S.N. Smirnov, N.S. Golubev, G.S. Denisov, H. Benedict, P. Schah-Mohammedi, H.H. Limbach, Hydrogen/Deuterium isotope effects on the NMR chemical shifts and geometries of intermolecular low-barrier hydrogen-bonded complexes, J. Am. Chem. Soc. 118 (1996) 4094–4101.
[42] G. Zhao, K. Han, Y. Lei, Y. Dou, Ultrafast excited-state dynamics of tetraphenylethylene studied by semiclassical simulation, J. Chem. Phys. 127 (2007) 094307http://doi.org/10.1063/1.2768347.
[43] G. Zhao, F. Yu, M. Zhang, N. BrianH, H. Yang, K. Han, P.J. Stang, Substituent effects on the intramolecular charge transfer and fluorescence of bimetallic platinum complexes, J. Phys. Chem. A 115 (2011) 6390–6393 http://doi.org/10.1021/jp202825q.
[44] Y. Niu, Q. Peng, C. Deng, X. Gao, Z. Shuai, Theory of excited state decays and optical spectra: application to polyatomic molecules, J. Phys. Chem. A 114 (2010) 7817–7831 http://doi.org/10.1021/jp101568f.
[45] Y. Niu, Q. Peng, Z. Shuai, Promoting-mode free formalism for excited state radiation less decay process with Duschinsky rotation effect, Sci. China Ser. B Chem. 51 (2008) 1153–1158 http://doi.org/10.1007/s11426-008-0130-4.